Al-Rafidain J Med Sci. 2024;6(2):94-100
DOI: https://doi.org/10.54133/ajms.v6i2.728

A J M S
Online ISSN (2789-3219)

Research Article

Preparation and Effects of Manganese Oxide Nanoparticles Against Quinolone-Resistant Bacteria Isolated from Hospital Wastewater

Mohammed Fadhil AboKsour*, Mohammed Faraj Al Marjani, Ahmed Mahdi Rheima

[1]*Department of Microbiology, College of Science, Mustansiriyah University, Baghdad, Iraq*

Received: 11 March 2024; Revised: 6 May 2024; Accepted: 11 May 2024

Abstract

Background: The widespread administration of quinolones may have led to an increase in bacterial resistance development. ***Objective***: To synthesize and characterize manganese oxide nanoparticles (MnO2NPs) and evaluate their effects on the viability and biofilm formation of quinolone-resistant gram-positive and negative pathogenic bacteria. ***Methods***: We prepared MnO2NPs using the photo-irradiation method and recorded their characteristics using XRD, TEM, and SEM. *Staphylococcus aureus*, *Streptococcus pneumonia*, *Escherichia coli*, *Klebsiella pneumonia*, and *Pseudomonas aeruginosa* were collected from the wastewater of Baghdad hospitals during the period from July 3rd to July 14th, 2023. We used the VITEK2 system to confirm and identify all of the isolates. We conducted biofilm formation and antibiotic susceptibility tests using nalidixic acid, ciprofloxacin, norfloxacin, aztreonam, levofloxacin, and ofloxacin, and also detected the qnrA and qnrB genes. Finally, we evaluated the effects of the prepared nanoparticles on the viability and biofilm formation of bacterial isolates. ***Results***: MnO2NPs characterizations showed a diffraction peak at 2θ values with 21 nm average sizes; *qnrA* and *qnrB* genes were found in three and four isolates, respectively; and significant effects of MnO_2NPs against viability and biofilm formation were recorded. ***Conclusions***: The synthesized nanoparticles have antibacterial and anti-biofilm activities against a variety of bacteria possessing *qnr* genes. Even multi-resistant bacterial isolates have the potential to be strong antimicrobial agents against these pathogens.

Keywords: Antibacterial activity, Antibiofilm effect, Bacterial resistance, MnO_2NPs.

تحضير وتأثيرات جسيمات أكسيد المنغنيز النانوية ضد البكتيريا المقاومة للكينولون المعزولة من مياه الصرف الصحي في المستشفيات

الخلاصة

الخلفية: قد يكون إعطاء الكينولونات على نطاق واسع قد أدى إلى زيادة في تطور المقاومة البكتيرية. **الهدف**: توليف وتوصيف جسيمات أكسيد المنغنيز النانوية وتقييم آثارها على صلاحية وتكوين الأغشية الحيوية للبكتيريا المسببة للأمراض إيجابية الجرام والسالبة المقاومة للكينولون. **الطرق**: قمنا بإعداد MnO_2NPs باستخدام طريقة التشعيع الضوئي وسجلنا خصائصها باستخدام XRD و TEM و SEM. تم جمع المكورات العنقودية الذهبية والالتهاب الرئوي العقدية والإشريكية القولونية والالتهاب الرئوي الكلبسيلة والزائفة الزنجارية من مياه الصرف الصحي لمستشفيات بغداد خلال الفترة من 3 تموز إلى 14 تموز 2023. استخدمنا نظام VITEK2 لتأكيد وتحديد جميع العزلات. أجرينا اختبارات تكوين الأغشية الحيوية والحساسية للمضادات الحيوية باستخدام حمض الناليديكسيك وسيبروفلوكساسين والنورفلوكساسين والأستريونام والليفوفلوكساسين وأوفلوكساسين، واستكشفنا أيضا جينات *qnrA* و qnrB. أخيرا، قمنا بتقييم آثار الجسيمات النانوية المحضرة على صلاحية العزلات البكتيرية وتكوينها الغشاء الحيوي. **النتائج**: أظهرت توصيفات MnO2NPs ذروة حيود عند قيم θ2 بمتوسط أحجام 21 نانومتر. تم العثور على جينات *qnrA* و *qnrB* في ثلاث وأربع عزلات، على التوالي. وتم تسجيل تأثيرات كبيرة ل MnO_2NPs ضد الجدوى وتكوين الأغشية الحيوية. **الاستنتاجات**: الجسيمات النانوية المركبة لها أنشطة مضادة للبكتيريا ومضادة للغشاء الحيوي ضد مجموعة متنوعة من البكتيريا التي تمتلك جينات *qnr*. حتى العزلات البكتيرية متعددة المقاومة لديها القدرة على أن تكون عوامل قوية مضادة للميكروبات ضد مسببات الأمراض هذه.

* ***Corresponding author***: Mohammed F. AboKsour, Department of Microbiology, College of Science, Mustansiriyah University, Baghdad, Iraq; Email: m.aboksour@uomustansiriyah.edu.iq

Article citation: AboKsour MF, Al Marjani MF, Rheima AM. Preparation and Effects of Manganese Oxide Nanoparticles Against Quinolone-Resistant Bacteria Isolated from Hospital Wastewater. *Al-Rafidain J Med Sci*. 2024;6(2):94-100. doi: https://doi.org/10.54133/ajms.v6i2.728

© 2024 The Author(s). Published by Al-Rafidain University College. This is an open access journal issued under the CC BY-NC-SA 4.0 license (https://creativecommons.org/licenses/by-nc-sa/4.0/).

INTRODUCTION

Antibiotic resistance is becoming an increasingly serious public health issue. In recent years, the rise of antibiotic-resistant bacterial species has posed a serious challenge to public health, making effective disease treatment more difficult around the world. In recent decades, the frequency of microbial illnesses has increased dramatically [1]. The rapid rise of antibiotic-resistant bacterial species has greatly hampered clinical treatment around the world. These newly resistant strains have rendered microorganisms impervious to standard antimicrobial therapy, resulting in disease persistence, increased healthcare expenses, and an increased mortality risk [2]. In recent decades, various novel antibiotics have been developed that have demonstrated improved efficiency against multidrug-resistant microorganisms. As a result, alternate therapy agents are critical for addressing the difficulties associated with these drug-resistant disorders [1]. Nanoparticle technology has emerged in recent decades, allowing for the development of dependable sensors with a wide range of applications, as well as nanoparticle-based antibacterial treatments [4]. Furthermore, nanoparticles have the potential to extend the limitations of conventional antibacterial medications. Nanoparticles that operate as antibiotics are gaining popularity due to their potential to overcome the limits of regular antibiotics. They are very efficient against multidrug-resistant mutants and biofilms [5]. Biofilms, which are organized aggregates of bacteria, can withstand a variety of environmental conditions and are resistant to antibiotics [6]. Biofilms are clusters of bacteria embedded in an extracellular polymeric substance, mostly consisting of nucleic acids, polysaccharides, and proteins [6]. Antibiotic inefficacy in non-treating biofilm infections, due to a permeability barrier, may provide hurdles to long-term disease eradication [1]. New antibiofilm agents are required to treat illnesses caused by bacteria that form biofilms [6]. Biofilms are clusters of bacteria embedded in an extracellular polymeric substance, mostly consisting of nucleic acids, polysaccharides, and proteins [7]. Antibiotics' ineffectiveness in treating biofilm infections, owing to a permeability barrier, may provide hurdles to long-term disease eradication [8]. To treat infections caused by bacteria that form biofilms, novel antibiofilm agents are required [7,8]. Metal oxide nanoparticles have high antibacterial capabilities and are compatible with mammals, making them effective agents [9]. There is evidence that MgO nanoparticles can kill both gram-positive and gram-negative bacteria, such as *Streptococcus pneumonia* and *E. coli* [8]. The current study aimed to synthesize and analyze manganese oxide nanoparticles, as well as assess their impact on the survival and biofilm formation of resistant gram-positive and gram-negative bacteria.

METHODS

Synthesis of oxide nanoparticles

All compounds were analyzed and used without further processing. Manganese oxide (MnO_2NPs) manufactured using reported methods [10,11] provided manganese nitrate [$Mn(NO_3)_2$] and oxalic acid [$C_2H_2O_4$] (Figure 1).

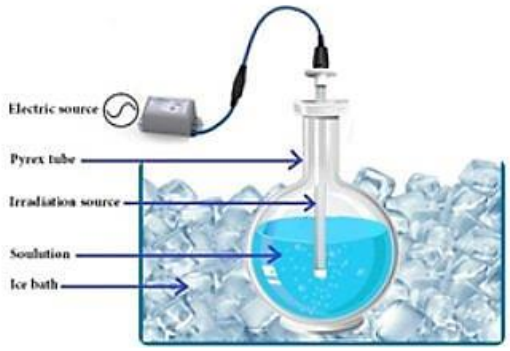

Figure 1: Photo-irradiation of synthesized MnO_2NPs

The photocell requires a 125 W UV mercury lamp with a wavelength of 365 nm and an ice bath-cooled tube to prevent temperature rise caused by UV radiation. As a result, 2 moles of nitrate were dissolved in 25 ml of water, followed by 4 moles and 25 ml of oxalic acid, which was gently added to the solution over 60 minutes. The solution was irradiated, and a dark grain precipitated. A water-filled centrifuge was used to separate and wash them multiple times. The powder was dried overnight at 60 ºC and calculated in a furnace at 450 ºC for 4 hours, resulting in a dark precipitate of MnO_2 NPs.

Characterization of MnO_2 NPs

X-ray diffraction (XRD) tests were done with a Japan (XRD-6000) rotating anode X-ray tube that was filled with Cu K (λ = 1.52A˚). To capture images, we used a JEOL JEM-2100 transmission electron microscope with a 100 kV acceleration voltage. We obtained the MnO2 NPs' moral using scanning electron microscopy (SEM; JEOL JEM-6510 LV) with a gold layer [12,13].

Bacterial isolates

Bacterial isolates of *Staphylococcus aureus*, *Streptococcus pneumonia*, *Escherichia coli*, *Klebsiella pneumonia*, and *Pseudomonas aeruginosa* were obtained from the microbiology laboratories of Science at Mustansiriyah University. These isolates were collected from the wastewater of Baghdad hospitals during the period from July 3rd to July 14th, 2023. The VITEK2 system was used to identify all of the isolates according to the manufacturers' specifications.

Antimicrobial susceptibility pattern

Nalidixic acid, ciprofloxacin, norfloxacin, aztreonam, levofloxacin, and ofloxacin were tested for antimicrobial susceptibility using the disc diffusion method [14,15].

Detection of the qnrA and qnrB genes

After the cultivation of bacterial isolates in Luria-Bertani broth at 37 °C for 18 hours, several colonies of bacteria were transferred to distilled water. The bacterial DNA of all isolates was extracted by using the boiling method [16]. Multiplex PCR was done by using four primers, as shown in Table 1.

Table 1: *qnrA* and *qnrB* primers *PCR*

Primers	Primer sequence	Product size	Ref.
qnrA-F	5-ATTTCTCACGCCAGGATT-3	580 bp	16
qnrA-R	5-GATCGGCAAAGGTTAGGTCA-3		
qnrB-F	5-GATCGTGAAAGCCAGAAAGG-3	264 bp	
qnrB-R	5-ACGATGCCTGGTAGTTGTCC-3		

Five bacterial DNA, four primers (1 µl of each), ten of master mix (Jena, Germany), and one of deionized water were added to reach a final volume equal to 20 µl. The reaction was performed according to a previous study [17–19].

Determination of antibacterial effects

The antibacterial properties of MnO2NPs were tested against all of the selected bacterial isolates (*S. aureus*, *S. pneumonia*, *E. coli*, *K. pneumonia*, and *P. aeruginosa*) using the well diffusion method [18]. We diluted the overnight bacterial growth in sterilized distilled water until it met the McFarland criterion (1.5*10-8 CFU/ml). Loopfuls of the bacterial suspensions were inoculated on Moller-Hinton agar plates, 5 mm in diameter, with wells containing 62, 125, 250, 500, 1000, and 2000 µg/ml of MnO2NPs. The plates were then incubated at 37 ºC for 24 hours to determine the effectiveness of the MnO_2NPs in killing the chosen isolates. Distilled water served as a negative control. MnO_2NPs were serially diluted from 62 to 2000 µg/ml, with 100 µl each added to three wells. In addition, 80 µl of each Muller-Hinton broth suspension was put into the 96-well plate. After 24 hours of incubation at 37 ºC, the minimum inhibitory concentrations of MnO2NPs were measured. In test conditions, these nanoparticles can arrest bacterial growth or kill the bacteria. Wells without MnO_2NPs and others without microorganisms served as positive and negative controls, respectively.

Determination of MnO_2NPs antibiofilm effects

Effects of the prepared MnO_2NPs against biofilm formation of the collected bacterial isolates were performed according to previous studies [21,22].

Statistical analysis

SPSS software (IBM, Chicago, IL, USA) version 20 was used for the statistical analysis. Fisher's test and the chi-square test were used in this study, and a *p*-value of less than 0.05 was considered statistically significant.

RESULTS

Figure 2 displays the XRD patterns of MnO_2NPs. The XRD pattern's diffraction peaks are all indexed to oxide, in accordance with JCPDS 24-0735. The XRD pattern of MnO_2NPs displayed diffraction peaks of 28.6°, 37.2°, 41.0°, 42.8°, 46.0°, 56.6°, 59.3°, 67.2°, and 72.2 at 2θ values indexed to 110, 101, 200, 111, 210, 211, 220, and 310, due to the tetragonal structure of MnO_2.

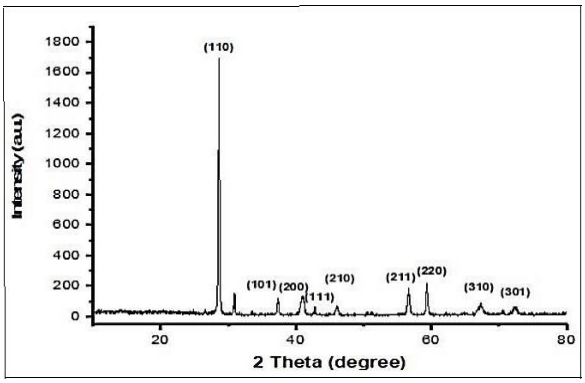

Figure 2: XRD pattern of the MnO_2NP

Figures 3A and B show TEM images of nanoscale MnO_2. The MnO_2NPs have an average size of around 21 nm, and figures 4A and B show SEM images utilized to analyze the surface structures of photochemically generated MnO_2NPs.

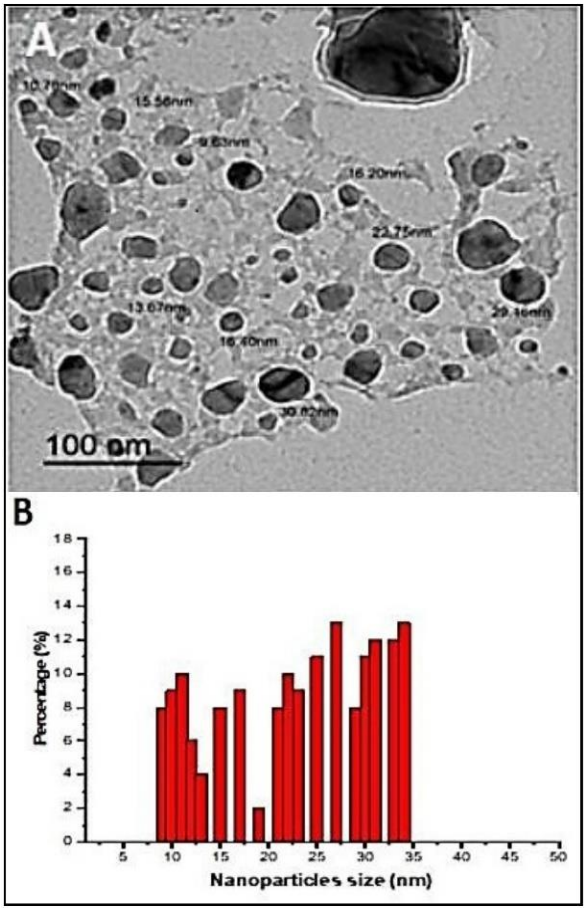

Figure 3: A) TEM image of photochemically synthesized MnO_2NPs. B) Distribution of MnO_2NPs

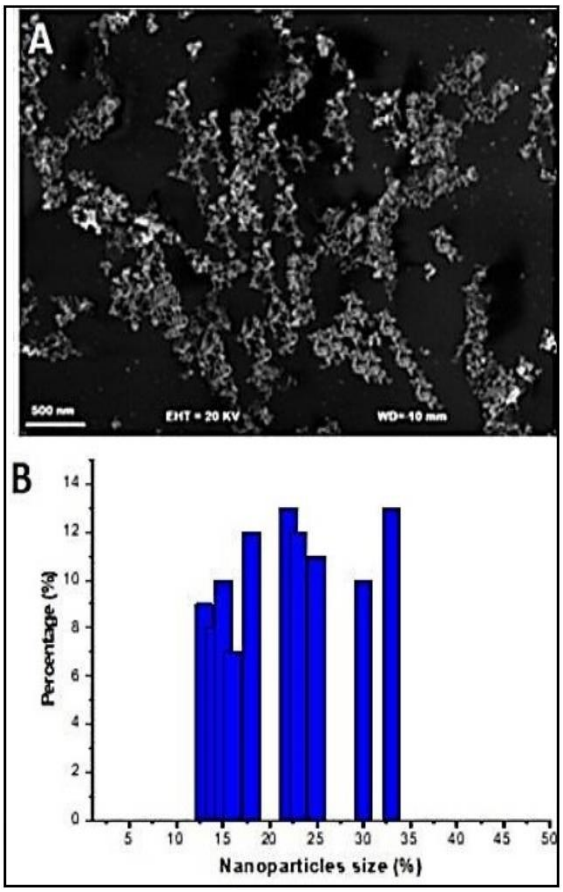

Figure 4: A) SEM image of MnO_2NPs**.** B) Distribution of MnO_2NPs by SEM image

The susceptibility tests revealed that all the isolates were resistant to three or more quinolones. Nalidixic acid demonstrated the highest resistance (80%), followed by ofloxacin and ciprofloxacin, both with 60% resistance. Table 2 shows that levofloxacin had the lowest resistance rate (10%).

Table 2: Antimicrobial-susceptibility for bacterial isolates

Isolates	NA (30µg)	CIP (5µg)	NOR (10µg)	AZT (30µg)	LEV (5µg)	FX (5µg)
S. aureus	S	S	R	S	S	R
S. pneumoniae	R	R	R	R	S	S
E. coli	R	S	S	R	R	I
K. pneumoniae	R	R	R	S	I	I
P. aeruginosa	R	R	S	R	S	R
Resistance %	80	60	60	40	20	40

Multiplex PCR was utilized to successfully amplify the *qnrA* and *qnrB* genes. The selected bacterial isolates all had one or two of the *qnr* genes examined in the current investigations. Three isolates had the *qnrA* gene, whereas four isolates contained the qnrB gene. Generally, three of the five isolates had one of the qnr genes (*qnrA* or *qnrB*), whereas the other two had both (Figure 5). The antimicrobial effects of MnO_2NPs on tested bacterial isolates showed that 125 and 250 µg/ml concentrations affect all tasted bacteria, while 500 µg/ml showed weak activity against S. aureus and S. pneumonia without any recoded activity against the other isolates (see table 3).

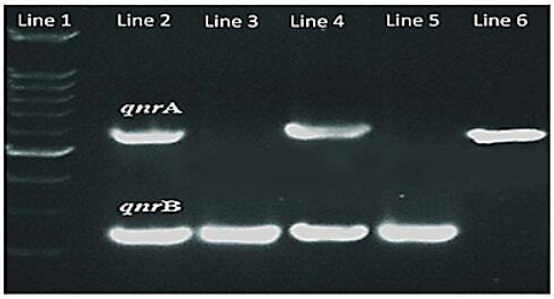

Figure 5: PCR product *qnrA* and *qnrB* genes on an agarose gel electrophoresis; where line 1: DNA ladder, line 2: *P. aeruginosa*, line3: *K. pneumonia*, line 4: *E. coli*, line 5: *S. pneumoniae*, and line 6: *S. aureus*.

Moreover, inhibitory zones of all isolates were observed by utilizing 2000 µg/ml of MnO_2NPs. In general, 2000 µg/ml of MnO_2-NPs was found to have the largest clear zone against *S. aureus* (21 mm) and the smallest clear zone against *P. aeruginosa* (12 mm), as shown in Table 3.

Table 3: Antimicrobial effect of MnO_2NPs against bacterial isolates and MIC values

Bacterial Species	Mn-NPs concentration (µg/ml)					
	125	250	500	1000	2000	MIC
S. aureus	0	0	8	14	21	250
S. pneumonia	0	0	7	12	18	>1000
E. coli	0	0	0	11	16	500
K. pneumonia	0	0	0	9	14	1000
P. aeruginosa	0	0	0	0	12	>1500

Conversely, the MnO_2NPs minimum inhibitory concentrations revealed the lowest MIC against *S. aureus* and the highest against *S. pneumonia*. Results MnO_2NPs strongly inhibited biofilm formation in all bacterial isolates at doses of 31.25, 62.5, and 125 µg/ml. *S. aureus* biofilm was the most affected, with a reduction in optical value from 1.5 to 0.9 (40%), while *P. aeruginosa* was the least affected, with a reduction of 7.6% and an optical value of 1.7 to 1.58 (Figure 6).

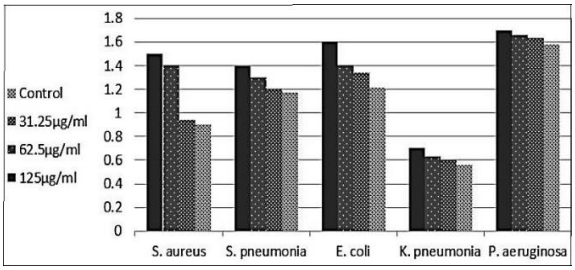

Figure 6: Antibiofilm activity of different concentrations of MnO_2NPs.

DISCUSSION

The purity of the nanosample and the lack of contaminants were the most critical factors in obtaining the MnO_2NPs. According to the Debye-Scherrer formula, the crystal size was determined to be 16.4 nm [23,24]. The TEM image clearly demonstrates that MnO_2NP sample spherical particles are composed of a decent percentage of crystals and have a restricted distribution [25].

Furthermore, the TEM results of the MnO_2NPs sample reveal particle aggregation into a porous block [26]. Figures 4A and B show the surface architectures of photochemically produced MnO_2NPs as studied using a scanning microscopy electron (SEM). The illustration illustrates that the spherical particles and crystal structures created are the primary components, demonstrating that MnO_2NPs do not aggregate. The SEM measurement revealed zero dimensions and particle formation, as all constructed particle measurements were significantly smaller than 100 nm [27]. Over the last few decades, five specific bacterial isolates have been identified as one of the world's main causes of nosocomial infections [28]. The *qnr* genes produce proteins that allow bacteria to withstand various antibiotics that are not quinolones. Even though *qnr* genes are one of the most resistant agents to quinolone derivatives, their prevalence has recently increased drastically [29]. The isolates in the current investigation were highly resistant to nalidixic acid (80%), with the lowest resistance found against levofloxacin (10%). As a result, nalidixic acid appears to be an unsuitable therapy for these bacteria. Furthermore, because levofloxacin is rarely used in clinical practice, it could be a useful treatment. Surprisingly, most of the isolates were resistant to all quinolone antibiotics [29,30]. This could indicate that the medicine is being used recklessly and incorrectly. According to a prior study, the rate of quinolone resistance is significantly higher here than in other parts of the world [30]. *Qnr* genes were discovered in a significant percentage of isolates in the current investigation, with qnrA at 60%, *qnrB* at 80%, and two of these resistance genes at 40%. In terms of quinolone resistance, the *qnrB* gene is more essential than qnrA. Additional variables, such as efflux pump overexpression, lower amounts of chemicals within cells, and mutations in enzymes such as topoisomerase IV and DNA gyrase, may also be successful in producing the same result [31]. However, quinolones are the most commonly prescribed antibiotics for the treatment of urinary tract infections. In today's world, the possibility of therapy ineffectiveness among Iranian patients is a major worry. [32]. Manganese nanoparticles were examined for their antibacterial effectiveness against two gram-positive bacteria (*S. aureus* and *S. pneumoniae*) and three gram-negative bacteria (*E. coli*, *K. pneumoniae*, and *P. aeruginosa*). The zone of inhibition was compared to that of a popular commercial antibiotic. We used both quantitative and qualitative assays to determine the antibacterial activity of the selected isolates. There is little question about the inhibitory zone surrounding the MnO_2NP wells, which indicates that the nanoparticles are killing the bacterium isolates. Other experiments found that MnO_2NPS had a significant impact on antibacterial activity [33]. The poor efficacy against P. aeruginosa could be attributed to the bacteria's advanced cell wall structure, which contains a high percentage of virulence factors and resistance mechanisms, or it could be because the OH produced by MnO_2NPs was insufficient to damage the cell wall. Antimicrobial activity against bacterial isolates was observed at high doses in the current study [34]. Furthermore, the particular mechanism of bacterial resistance remains unknown. MnO_2NPs interact with the membrane, causing membrane changes that appear as pits on the membrane surfaces and subsequently lead to the formation of pores, resulting in cell death [33,35]. It is also likely that MnO_2NPs were effective against quinolone-resistant bacteria via this method. When the concentration of nanoparticle metals in the culture medium rises, so does the interaction between oxygen and the dehydrogenase enzyme, resulting in increased antimicrobial activity. Another possible explanation is the abrasive surface roughness of MnO_2NPs, which is induced by metal oxide and/or transition metal doping, which promotes surface defects [36]. MnO_2NPs had MICs against both gram-negative and gram-positive bacteria strains [37]. Gram-positive bacterial strains were more susceptible to the NPs tested in this investigation than gram-negative strains. Numerous studies have also demonstrated the beneficial effects of MnO_2NPs on gram-positive bacteria [38]. High activity against gram-positive bacteria may be due to differences in cell walls, or because peptidoglycan is more abundant in gram-positive bacteria than in negative bacteria, or due to electrostatic interactions between NPs and the cell surface that result in morphological changes in gram-negative bacteria, increasing cell permeability and NP accumulation in the cytoplasm [39]. SoxR and oxyR are two regulators that activate genes involved in oxidative stress resistance mechanisms. SoxR reacts to superoxide anions, whereas oxyR responds to hydrogen peroxide stress. Bacteria treated with silver nanoparticles (AgNPs) showed increased expression of genes linked with oxidative stress resistance. These genes include *soxR*, *oxyR*, *sodA*, *sodB*, and *sodC*, which produce superoxide dismutase, an enzyme that converts superoxide to hydrogen peroxide. Furthermore, the *katE* and *katG* genes were deregulated, which are involved in the conversion of hydrogen peroxide to oxygen. [40]. Bacterial resistance to nanoparticles is attributed to changes in gene expression and oxidative stress, which results in a reduction in porins, activation of redox-sensitive transcriptional activators known as SOXR and OXYR [41], modification in the electrical charge of the bacterial wall, increased expression of efflux systems, and a change in lipopolysaccharide synthesis [42]. Finally, because bacterial pathogenicity is heavily dependent on biofilm formation and swarming movement, a significant reduction in bacterial biofilm formation contributes to successful pathogenic suppression while also lowering virulence factors [43].

Study limitations

There are two limitations to this investigation. The first limitation is the study's limited sample size of bacterial species. The second is the failure to apply the prepared nanoparticles against fungal or parasitic pathogens.

Conclusion

In this study, we effectively produced MnO_2NPs. According to the inhibition zone data, synthesized MnO_2NPs inhibit gram-positive bacteria more effectively than gram-negative bacteria. As a result, even multi-resistant bacterial isolates have the potential to serve as potent antimicrobial agents against this pathogenic infection. Effective antibiotic stewardship is especially important in healthcare settings. We need a more detailed investigation to assess the prevalence of quinolone resistance in Baghdad and address its spread to other nosocomial infections.

ACKNOWLEDGMENTS

The authors thank the Mustansiriyah University for providing the essential facilities and financial assistance for this study. They also thank all colleagues for their assistance.

Conflict of interests

No conflict of interests was declared by the authors.

Funding source

The authors did not receive any source of fund.

Data sharing statement

Supplementary data can be shared with the corresponding author upon reasonable request.

REFERENCES

1. AboKsour MF, Al-Jubori SS, Jawad HA. Influence of Helium-Neon laser on some virulence factors of *Staphylococcus aureus* and *Escherichia coli*. *Al-Mustansiriyah J Sci*. 2018;9(3):29. doi: 10.23851/mjs.v29i3.619.
2. Zeng W, Xu W, Xu Y, Liao W, Zhao Y, Zheng X, et al. The prevalence and mechanism of triclosan resistance in Escherichia coli isolated from urine samples in Wenzhou, China. *Antimicrob Resist Infect Control*. 2020;9(1):161. doi: 10.1186/s13756-020-00823-5.
3. Atmanto Y, Adi K, Abd Kadir N, Rusli B. Extended spectrum beta lactamase (ESBL) confirmation test using E-Test. *Int J Recent Adv Multidiscipl Topics*. 2022:5;125-130.
4. Adarsha JR, Ravishankar TN, Ananda A, Manjunatha CR, Shilpa BM, Ramakrishnappa T. Hydrothermal synthesis of novel heterostructured Ag/TiO_2 /$CuFe_2O_4$ nanocomposite: Characterization, enhanced photocatalytic degradation of methylene blue dye, and efficient antibacterial studies. *Water Environ Res.* 2022;94(6):e10744. doi: 10.1002/wer.10744.
5. Chen SC, Kuo TY, Lin HC, Chen RZ, Sun H. Optoelectronic properties of p-type NiO films deposited by direct current magnetron sputtering versus high power impulse magnetron sputtering. *Appl Surf Sci.* 2020;50(8):14-19. doi:10.1016/j.apsusc.2019.145106.
6. Flemming H, Wingender J, Szewzyk U, Steinberg P, Rice S A, Kjelleberg S. Biofilms: an emergent form of bacterial life. *Nat. Rev. Microbio.* 2016;9(14):563–575. doi: 10.1038/nrmicro.2016.94.
7. Mohamed K, Zine K, Fahima K, Abdelfattah E, Sharifudin SM, Duduku K. NiO nanoparticles induce cytotoxicity mediated through ROS generation and impairing the antioxidant defence in the human lung epithelial cells (A549): Preventive of Pistacia lentiscus essential oil. *Toxicol Rep*. 2018:5;480–488. doi: 10.1016/j.toxrep.2018.03.012.
8. da Silva B, Paiva Abuçafy M, Manaia B, Junior J, Chiari-Andréo B, Pietro R, et al. Relationship between structure and antimicrobial activity of zinc oxide nanoparticles: An overview. *Int J Nanomed*. 2019:14; 9395–9410. doi: 10.2147/IJN.S216204.
9. Ramalingam V, Sundaramahalingam S, Rajaram R. Size-dependent antimycobacterial activity of titanium oxide nanoparticles against Mycobacterium tuberculosis. *J Mater Chem.* 2019;7:4338–4346. doi: 10.1039/C9TB00784A.
10. Kannan K, Radhika D, Sadasivuni KK, Reddy KR, Raghu AV. Nanostructured metal oxides and its hybrids for photocatalyticand biomedical applications. *Adv Col Int Sci.* 2020;281:102178. doi: 10.1016/j.cis.2020.102178.
11. Shkir M, Yahia IS, Ganesh V, Bitla Y, Ashraf IM, Kaushik A, *et al*. A facile synthesis of Au-nanoparticles decorated PbI_2 single crystalline nanosheets for optoelectronic device applications. *Sci Rep*. 2018;8(7):13806. doi: 10.1038/s41598-018-32038-5.
12. Rheima AM, Al Marjani MF, Aboksour MF, Hashim SM. Evaluation of anti-biofilm formation effect of nickel oxide nanoparticles (NiO-NPs) against methicillin-resistant *Staphylococcus aureus* (MRSA). *Int J of Nanosci Nanotechnol*. 2021;17(4):221-230. doi: ijnnonline.net/article_247640.html.
13. Mohammed FA. Presence of extended-spectrum β-Lactamases genes in *E. coli* isolated from farm workers in the South of London. *IJPQA* 2018;9(1):64-67 doi: 10.25258/ijpqa.v9i01.11361.
14. Humphries R, Bobenchik AM, Hindler JA, Schuetz AN. Overview of changes to the clinical and laboratory standards institute performance standards for antimicrobial susceptibility testing. *J Clin Microbiol*. 2021;59(12):e0021321. doi:10.1128/jcm.00213-21.
15. Sirelkhatim A, Mahmud S, Seeni A, Kaus NHM, Ann LC, Bakhori SKM, et al. Review on zinc oxide nanoparticles: Antibacterial activity and toxicity mechanism. *Nanomicro Lett*. 2015;7(3):219-242. doi: 10.1007/s40820-015-0040-x.
16. Rodríguez JM, Cano ME, Velasco C, Martínez L, Pascual Á. Plasmid-mediated quinolone resistance: an update. *J Infect Chemother*. 2021;17(2):149-182. doi: 10.1007/s10156-010-0120-2.
17. Saki M, Farajzadeh Sheikh A, Seyed-Mohammadi S, Asareh Zadegan Dezfuli A, Shahin M, Tabasi M, et al. Occurrence of plasmid-mediated quinolone resistance genes in Pseudomonas aeruginosa strains isolated from clinical specimens in southwest Iran: a multicentral study. *Sci Rep.* 2022;12(1):2296. doi: 10.1038/s41598-022-06128-4.
18. Nsofor CM, Tattfeng MY, Nsofor CA. High prevalence of qnrA and qnrB genes among fluoroquinolone-resistant *Escherichia coli* isolates from a tertiary hospital in Southern *Nigeria. Bull Natl Res Cent.* 2021;45(26):2-7. doi: 10.1186/s42269-020-00475-w.
19. Esmaeel NE, Gerges MA, Hosny TA, Ali AR, Gebriel MG. Detection of chromosomal and plasmid-mediated quinolone resistance among Escherichia coli isolated from urinary tract infection cases; Zagazig University Hospitals, Egypt. *Infe Dru Resist*. 2020:13;413–421. doi: 10.2147/IDR.S240013.
20. Mayers DL, Lerner SA, Ouelette M. Antimicrobial drug resistance C: Clinical and Epidemiological Aspects; *Sprin Dor Heid*. 2019;681–1347. doi: 10.1007/978-1-60327-595-8.
21. Martin I, Sawatzky P, Liu G. Antimicrobial resistance to *Neisseria gonorrhoeae* in Canada: 2009–2013. *Can Commun Dis Rep.* 2015: 41(2):35-41. doi: 10.14745/ccdr.v41i02a04.
22. Mabona U, Viljoen A, Shikanga E. Antimicrobial activity of Southern African medicinal plants with dermatological relevance: from an ethno pharmacological screening approach, to combination studies and the isolation of a bioactive compound. *J Ethnopharmacol.* 2013;148(1):45–55. doi: 10.1016/j.jep.2013.03.056.
23. Fahs A, Quiles F, Jamal D, Humbert F, Francius G. In situ analysis of bacterial extracellular polymeric substances from a *Pseudomonas fluorescens* biofilm by combined vibrational and single molecule force spectroscopies. *J Phys Chem.* 2014;118(24):6702-6713. doi: 10.1021/jp5030872.
24. Rabiei M, Palevicius A, Monshi A, Nasiri S, Vilkauskas A, Janusas G. Comparing methods for calculating nano crystal size of natural hydroxyapatite using X-ray diffraction. *Nanomaterials*. 2020;10(9):1627. doi: 10.3390/nano10091627.

25. Altammar KA. A review on nanoparticles: characteristics, synthesis, applications, and challenges. *Fron Microbiol.* 2023;17(14):115-126. doi: 10.3389/fmicb.2023.1155622.
26. Islam F, Shohag S, Uddin MJ, Islam MR, Nafady MH, Akter A, *et al.* Exploring the journey of zinc oxide nanoparticles (ZnO-NPs) toward biomedical applications. *Materials*. 2022;15(6):2160. doi: 10.3390/ma15062160.
27. Khan I, Saeed K, Khan I. Nanoparticles: Properties, applications and toxicities. *Arab J Chem.* 2019;12(7): 908–931. doi: 10.1016/j.arabjc.2017.05.011.
28. Kučuk N, Primožič M, Knez Ž, Leitgeb M. Sustainable biodegradable biopolymer-based nanoparticles for healthcare applications. *Int J Mol Sci*. 2023;24(4):3188. doi: 10.3390/ijms24043188.
29. Abid H, Mohd J, Ravi PS, Shanay R, Rajiv S. Applications of nanotechnology in medical field: a brief review. *Glob Health J*. 2023;7(2):70-77. doi: 10.1016/j.glohj.2023.02.008.
30. AboKsour MF, Shafiq SA, Mussa AH. An Evaluation of water pollution in the Southern Iraqi marshes by using bacterial indicators and other related parameters. *J Glog Pharm Technol*. 2017;10(9):412-418.
31. Zhao YC, Sun ZH, Xiao MX, Li JK, Liu HY, *et al.* Analysing the correlation between quinolone-resistant Escherichia coli resistance rates and climate factors: A comprehensive analysis across 31 Chinese provinces. *Environ Res.* 2024;245:117995. doi: 10.1016/j.envres.2023.117995.
32. Murray BO, Flores C, Williams C, Flusberg DA, Marr EE, Kwiatkowska KM, *et al.* Recurrent urinary tract infection: a mystery in search of better model systems. *Fron Cell Infect Microbiol.* 2021;11:691210. doi: 10.3389/fcimb.2021.691210.
33. Qamar U, Aatika M. Impact of climate change on antimicrobial resistance dynamics: an emerging One Health challenge. *Future Microbiol*. 2023;18:535-539. doi:10.2217/fmb-2023-0022.
34. Du T, Chen S, Zhang J, Li T, Li P, Liu J, et al. Antibacterial activity of manganese dioxide nanosheets by ROS-mediated pathways and destroying membrane integrity. *Nanomaterials (Basel)*. 2020;10(8):1545-58. doi: 10.3390/nano10081545.
35. Zaki A, Siddiqui MR, Khan SA. Use of manganese oxide nanoparticle (MnO_2NPs) and *Pseudomonas putida* for the management of wilt disease complex of carrot. Experimental Parasitology. *Exp Parasitol*. 2024;257:108698. doi: 10.1016/j.exppara.2024.108698.
36. Peymani A, Farivar TN, Najafipour R, Mansouri S. High prevalence of plasmid-mediated quinolone resistance determinants in *Enterobacter cloacae* isolated from hospitals of the Qazvin, Alborz, and Tehran provinces, Iran. *Rev Soc Bras Med Trop*. 2016;49(3):286–291. doi: 10.1590/0037-8682-0454-2015.
37. Tageldin M, Babier AM, Elhasan OA, Yousif M, Ahemir SY, Hussien, HM. *et al*. Molecular Detection of Plasmid-Mediated Quinolone Resistance Genes (qnrA and aac(6′)-Ib-cr) in Drug Resistant *Escherichia coli*, Sudan. *Microb Res J Int.* 2023;33(4):14-21. doi: 10.9734/mrji/2023/v33i41375.
38. Song Z, Wu Y, Wang H, Han H. Synergistic antibacterial effects of curcumin modified silver nanoparticles through ROS-mediated pathways. *Mater Sci Eng C Mater Biol Appl*. 2019;99:255-263. doi: 10.1016/j.msec.2018.12.053.
39. Zheng H, Ji Z, Roy KR, Gao M, Li R. Engineered graphene oxide nanocomposite capable of preventing the evolution of antimicrobial resistance. *ACS Nano*. 2019:13:11488–11499. doi: 10.1021/acsnano.9b04970.
40. Fan W, Bu W, Shen B, He Q, Cui Z, Liu Y, et al. Intelligent MnO_2 nanosheets anchored with upconversion nanoprobes for concurrent pH-/H_2O_2 -responsive UCL imaging and oxygen-elevated synergetic therapy. *Adv Mater*. 2022:27;4155–4161. doi: 10.1002/adma.201405141.
41. Yang Q, Wang X, Peng H, Arabi M, Li J, Xiong H, et al. Ratiometric fluorescence and colorimetry dual-mode assay based on manganese dioxide nanosheets for visual detection of alkaline phosphatase activity. Sens. *Actuat. B Chem.* 2020:302:127176. doi: 10.1016/j.snb.2019.127176.
42. Chen SC, Kuo TY, Lin HC, Chen R Z, Sun H. Optoelectronic properties of p-type NiO films deposited by direct current magnetron sputtering versus high power impulse magnetron sputtering. *Appl Surf Sci*. 2020:508, 145106. doi:10.1016/j.apsusc.2019.145106.
43. Song Z, Wu Y, Wang H, Han H. Synergistic antibacterial effects of crcumin modified silver nanoparticles through ROS-mediated pathways. *Mater Sci Eng C Mater Biol Appl*. 2019;99:255-263. doi: 10.1016/j.msec.2018.12.053.